

# Energy-Efficient NOMA Multicasting System for 5G Cellular V2X Communications with Imperfect CSI

Asim Ihsan, Wen Chen, Shunqing Zhang, and Shugong Xu

**Abstract**—Vehicle-to-everything (V2X) is a modern vehicular technology that improves conventional vehicle systems in traffic and communications. V2X communications demand energy-efficient and high-reliability networking because of massive vehicular connections and high mobility wireless channels. Non-orthogonal multiple access (NOMA) is a promising solution for 5G V2X services that intend to guarantee high reliability, quality-of-service (QoS) provisioning, and massive connectivity requirements. In V2X, it is vital to inspect imperfect CSI because the high mobility of vehicles leads to more channel estimation uncertainties. Unlike existing literatures, we propose energy-efficient roadside units (RSUs) assisted NOMA multicasting system for 5G cellular V2X communications, and investigate the energy-efficient power allocation problem. The proposed system multicast the information through low complexity optimal power allocation algorithms used under channel outage probability constraint of vehicles with imperfect CSI, QoS constraints of vehicles, and transmit power limits constraint of RSUs. The formulated problem with the channel outage probability constraint is a non-convex probabilistic optimization problem. This problem is solved efficiently by converting the probabilistic problem through relaxation into a non-probabilistic problem. Firstly, a low complexity gradient assisted binary search (GABS) method is adopted to obtain the optimal transmit power for each RSU. Subsequently, the successive convex approximation (SCA) technique is used that transforms the problem of power allocation factors of vehicles associated with its corresponding RSU into tractable concave-convex fractional programming (CCFP) problem. Then, the optimal solution is achieved through Dinkelbach and the dual decomposition method. The optimal power allocation through exhaustive search act as a benchmark, which has considerable computational complexity. Simulation results demonstrate that the proposed power allocation algorithm can obtain near-optimal energy efficiency (EE) performance with low computational complexity.

**Index Terms**—5G, Vehicular communication, Imperfect channel estimation, Power allocation, Energy efficiency, Multicasting.

## I. INTRODUCTION AND MOTIVATIONS

**I**N the last decade, there has been a rapid advancement in connected vehicles and their related technologies. Connected vehicles, which are also called V2X communications, emerge as an important integral part of the architecture of the intelligent transport system (ITS) [1]. V2X enables

many applications associated with vehicles, drivers, passengers, vehicles traffic, and pedestrians, which makes driving safer and more efficient for everyone. It includes vehicle-to-infrastructure (V2I), vehicle-to-pedestrian (V2P), vehicle-to-vehicle (V2V), and vehicle-to-network (V2N) communications. Through these communications, V2X can enhance traffic efficiency, road safety, and can provide entertainment services [2]. The energy management for building such a network is a challenging task because of many limiting factors such as explosive growth of connected vehicles, high mobility wireless channels, asynchronous transmissions, congested spectrum, and hardware imperfections. In vehicular networks, high mobility results in channel estimation errors, which affect the link reliability and system robustness [3]. Therefore, energy-efficient, high-reliability networking, and communications are essential for building ITS.

International standards are mandatory for the implementation of V2X communication systems. They provide specifications that ensure the interconnection between V2X systems and their components, and provide multi-vendor interoperability. Wireless access in vehicular environments (WAVE) standard is the core part of dedicated short-range communications (DSRC) technology, which has been installed on the roads in many countries since its release [4]. DSRC is a known technology for its robust performance in V2V communication and its ability to utilize the distributed channel access [5]. However, DSRC faces many challenges because of the design of its physical (PHY) and medium access control (MAC) layer. It can not match the low latency, the high bandwidth, and the network coverage requirement of future V2X applications, especially in dense environments [6]-[8]. Limitations of DSRC and current development in cellular technologies like LTE-V in 3GPP Release 14 [9], motivated researchers to investigate LTE based cellular V2X (C-V2X) communications. In C-V2X, numerous applications can be provided through two main types of connections, that is infrastructure-based communication (V2I/I2V) through the cellular interface and V2V communication through the PC5 interface. V2V communication is essential for safety applications, while infrastructure based communication plays a role in coordination. It is vital for the gathering of local or global real-time information such as data collections at remote RSUs for smart navigation and logistics, traffic management, and environmental monitoring. Then, provisioning real-time safety-related, location, and condition-based services, such as accident warning, intersection safety, speed limit information,

A. Ihsan and W. Chen are with Department of Information and Communication Engineering, Shanghai Jiao Tong University, Shanghai 200240, China. Email: {ihsanasim;wenchen}@sjtu.edu.cn.

S. Zhang and S. Xu are with School of Communications and Information Engineering, Shanghai University, Shanghai, China 200444. Email: {shunqing;shugong}@shu.edu.cn.

safe distance warning, traffic jam warning, and lane-keeping support besides the entertainment services [10]. These services can be provided to vehicles and other users in ITS through both base stations and RSU, which prevent accidents by delivering timely information. RSUs can be deployed on the roads with heavy data traffic, which can be an effective solution to alleviate the severe congestions in the cellular network [11].

5G mobile network plays a vital role in establishing V2X communications because it ensures the desired reliability, capacity, and low latency in exchanging information among vehicles [12], [13]. NOMA is an effective solution for providing low-latency and ultra-high reliability V2X services through 5G cellular networks. NOMA mitigates resource collisions because of its high overloading transmissions through limited resources [14], [15], thereby enhancing spectral efficiency and reducing latency for 5G V2X services [16], [17], [18]. Many researchers used NOMA in the vehicular networks to achieve ultra-high reliability and low-latency requirements [19], [20], [21]. Low-latency and high-reliability(LLHR) V2X broadcasting system for a dense network are proposed in [22]-[23]. This broadcasting system used a mixed centralized/distributed method based on NOMA. NOMA-spatial modulation (SM) is proposed in [24] to deal with the hostile V2V environment. It is proved that the bandwidth efficiency can be improved by using spatial modulation (SM) against channel correlation in multi-antenna V2V communication along with NOMA. A novel full-duplex(FD) decentralized V2X system based on NOMA is presented in [25], which meets the demands of massively connected vehicles and their various quality of services (QoS). Cooperative communication, in combination with NOMA as a broadcasting/multicasting scheme for 5G C-V2X communications, is used in [26]. The power allocation problem is formulated for half-duplex(HD) relay-aided and full-duplex(FD) relay-aided NOMA system, in which RSUs are considered as a relay for the base station.

Moreover, as the power domain is exploited in NOMA for multiple access, power allocation algorithms will greatly affect the performance of the NOMA systems. Power allocation in NOMA has been extensively studied. Most of the existing NOMA literatures focused on fixed power allocation algorithms [27]. The optimal global performance of NOMA can be realized through exhaustive search (ES) power allocation [28]. However, the complexity of the ES method is exponential [29]. The energy-efficient power allocation problem for V2X communications based on cellular D2D is proposed in [30]. In [31], authors presented an energy-efficient power allocation scheme for uplink relay assisted transmissions for V2X applications. The energy efficiency problem is formulated under transmit and circuit power constraints as well as delay constraints [32], [33], [34]. The power allocation problem for broadcasting/multicasting scheme based on cooperative NOMA for LLHR 5G C-V2X communications is formulated in [26] and [35]. They considered RSUs as relay in half-duplex(HD) mode in [35], while in both HD and FD mode in [26] for base station transmissions, and analyzed the power allocation problem for broadcasting/multicasting scheme with fairness among vehicles.

Inspired and motivated by the above research contributions,

the energy-efficient multicasting system for 5G V2X communications is proposed in this paper. Our major contribution is summarized as follows.

- *Energy efficient V2X multicasting system :*

Energy-efficient multicasting system for V2X communication is proposed in which multiple RSUs are assisting base station and multicast the information to their associated vehicles in their coverage. BS is installed with multiple antennas, which deal with each RSU as a beamforming group. Besides, the BS also deals with the vehicles directly in its vicinity. The proposed system achieves energy efficiency by obtaining the optimal transmit power for each RSU through GABS under channel outage probability constraint and RSU transmits power limit constraint. The probabilistic optimization problem under channel outage probability requirement constraint is transformed into a non-probabilistic optimization problem for the problem's efficient solution through approximation. Then, the energy-efficient power allocation problem for vehicles associated with RSU is formulated under QoS constraint. This non-convex problem is converted into a tractable CCFP problem through SCA, which is solved by Dinkelbach's and dual decomposition method.

- *Channel reliability :*

The proposed multicasting system is developed under the consideration of channel reliability constraint under imperfect CSI. In vehicular systems, the high mobility nature of vehicles results in more uncertainties in channel estimations, which affect link reliability and system robustness [36], [37], [38]. Therefore, it is necessary to inspect imperfect CSI in a vehicular environment [3]. For successful decoding and successive interference cancellation (SIC) at vehicles, the vehicles' transmission rate should not exceed their corresponding maximum achievable rate [26]. Therefore, the communication will stop if the transmission rate of the vehicles exceeds their corresponding achievable rate. The outage probability measures whether the transmission rate of vehicles exceeds the achievable rate [39]. It is a link/channel reliability constraint under imperfect channel estimation.

- *Low complexity :*

In the proposed multicasting system, RSUs are not utilizing their maximum transmit power all the time. Instead, they obtain their optimal energy efficiency under their transmit power limits. The optimal energy efficiency of RSUs is achieved through a low-complexity gradient assisted binary search (GABS) based iterative algorithm proposed in [40]. Then, power allocations factors for vehicles associated with RSU under their QoS constraints are obtained through low complexity iterative algorithm based on Dinkelbach's algorithm [41]. The obtained results for the proposed power allocation scheme are compared with optimal exhaustive search power algorithm (benchmark algorithm having high computational complexity) and is observed that our proposed power allocations scheme obtain near-optimal EE with low acceptable computational complexity for practical implementations.

The rest of the paper is organized as follows. Section II describes the system model and problem formulation with its solution for the proposed energy-efficient multicasting scheme for V2X communications. Section III presents the simulation results to verify the efficacy of the proposed algorithms. Section IV provides concluding remarks of the paper and future work.

## II. SYSTEM MODEL AND PROBLEM FORMULATION

### A. System Model

The system model for energy-efficient NOMA multicasting system is depicted in Fig. 1, in which the BS is deployed at the center of the system. BS is dealing  $B$  vehicles (denoted by  $\mathcal{B}-VUs$ ) in the regions where direct links between BS and vehicles are strong and can satisfy the QoS requirements. There are  $I$  RSUs in the system, where  $\mathcal{R} = \{RSU_i | i = 1, 2, 3, \dots, I\}$ . Each RSU is viewed as a relay with a single antenna, which deals with one group of vehicles (denoted by  $\mathcal{R}-VUs$ ) in its coverage in half-duplex decode-and-forward (DF) relaying mode. Each RSU can deal with  $K$  vehicles at a time. The vehicle  $k$  connected with  $RSU_i$  is denoted by  $\mathcal{V}_{k,i}$ . It is assumed that RSUs are deployed in the regions, where a direct link between the BS and vehicles associated with RSU is weak due to large path loss and can not fulfill the QoS requirement of vehicles. BS is operated with multiple antennas and zero-forcing technique and deals with each RSU as a beamforming group. The antenna array size at BS should be much more than the number of RSU and the beamforming group size, which results in the elimination of interference among RSUs. Consequently, the interference between different RSUs can be neglected. In the proposed system, for convenience, it is assumed that the transmission powers of  $\mathcal{B}-VUs$  are allocated equally by the BS, and the EE of the system is obtained through multiple RSUs.

In the multicasting scheme, vehicles associated with the same RSU requires different information from BS. Therefore NOMA is applied at RSUs to transmit the data in multicasting form [26]. Therefore, vehicles connected with the same RSU have interference among them, known as NOMA user interference, and they also have interference from  $\mathcal{B}-VUs$ , known as  $\mathcal{B}-VUs$  interference. In NOMA, interference from the vehicles with worse channel conditions associated with the same RSU can be removed through SIC technology. The interference cancellation from other vehicles is successful, if the signal-to-interference-plus-noise ratio (SINR) of a vehicle with large channel gain is greater than or equal to the SINR of a vehicle with inferior channel gain, for its own signal [42]. Without loss of generality, It is assumed that SINR of vehicles associated with  $RSU_i$  can be ordered as

$$\frac{|H_{k+1,i}|^2}{|G_{k+1,i}|^2 \sum_{b=1}^B P_b + \sigma^2} \geq \frac{|H_{k,i}|^2}{|G_{k,i}|^2 \sum_{b=1}^B P_b + \sigma^2}, \quad (1)$$

where,  $H_{k,i}$  and  $G_{k,i}$  are the channel coefficients from  $RSU_i$  to  $\mathcal{V}_{k,i}$  (information link) and BS to  $\mathcal{V}_{k,i}$  (interference link), respectively.  $P_b$  is the transmission power of the  $b^{th}$   $\mathcal{B}-VU$

from BS.  $\sigma^2$  is the variance of additive white Gaussian noise (AWGN). In NOMA, receivers are exploiting the SIC technique, therefore the signal received by  $\mathcal{V}_{k,i}$  can be expressed as

$$y_{k,i} = \underbrace{H_{k,i} \sqrt{P_i \alpha_{k,i}} s_{k,i}}_{\text{desired signal}} + \underbrace{H_{k,i} \sum_{m=k+1}^K \sqrt{P_i \alpha_{m,i}} s_{m,i}}_{\text{NOMA user interference}} + \underbrace{G_{k,i} \sum_{b=1}^B \sqrt{P_b} s_b}_{\mathcal{B}-VUs \text{ Interference}} + \underbrace{n_{k,i}}_{\text{noise}}, \quad (2)$$

where  $P_i$  is the total transmission power of the  $RSU_i$ ,  $\alpha_{k,i}$  and  $s_{k,i}$  represent the power allocation factor and the modulated symbol of  $\mathcal{V}_{k,i}$ , respectively.  $s_b$  is the transmitted modulated symbol of  $b^{th}$   $\mathcal{B}-VU$ .  $n_{k,i}$  denotes additive white Gaussian noise (AWGN) that has zero mean and variance ( $\sigma^2$ ).

The channel coefficients between  $RSU_i$ - $\mathcal{V}_{k,i}$  information link and BS- $\mathcal{V}_{k,i}$  interference link consist of the following components, respectively.

$$H_{k,i} = D_{k,i} \times h_{k,i}, \quad (3)$$

and

$$G_{k,i} = D'_{k,i} \times g_{k,i}, \quad (4)$$

where  $h_{k,i}$  and  $g_{k,i}$  are the fast fading component of the  $RSU_i$ - $\mathcal{V}_{k,i}$  information link and BS- $\mathcal{V}_{k,i}$  interference link, respectively.  $D_{k,i} = \sqrt{d_{k,i}^{-\beta} \vartheta_{k,i}}$  and  $D'_{k,i} = \sqrt{d'_{k,i}^{-\beta} \vartheta'_{k,i}}$ , where  $d_{k,i}$  and  $d'_{k,i}$  are the distance from the  $RSU_i$  to  $\mathcal{V}_{k,i}$  and BS to  $\mathcal{V}_{k,i}$ , respectively.  $\beta$  is the path-loss exponent.  $\vartheta_{k,i}$  and  $\vartheta'_{k,i}$  represent log normal shadowing random variable with 8 dB standard deviation for  $RSU_i$ - $\mathcal{V}_{k,i}$  information link and BS- $\mathcal{V}_{k,i}$  interference link, respectively.

The high mobility nature of vehicles results in channel estimation errors. The estimation of channel state information (CSI) of links is pilot based. By using the minimum mean square error (MMSE) channel estimation error model [39], [43], the rayleigh fading coefficients between  $RSU_i$ - $\mathcal{V}_{k,i}$  information link and BS- $\mathcal{V}_{k,i}$  interference link, respectively, can be modeled as

$$h_{k,i} = \hat{h}_{k,i} + \epsilon_{k,i}, \quad (5)$$

and

$$g_{k,i} = \hat{g}_{k,i} + \epsilon'_{k,i}, \quad (6)$$

where  $h_{k,i}$  and  $g_{k,i}$  are the accurate Rayleigh channel coefficients,  $\hat{h}_{k,i} \sim CN(0, 1 - \sigma_{RSU}^2)$  and  $\hat{g}_{k,i} \sim CN(0, 1 - \sigma_{BS}^2)$  are the estimated channel gains,  $\epsilon_{k,i} \sim CN(0, \sigma_{RSU}^2)$  and  $\epsilon'_{k,i} \sim CN(0, \sigma_{BS}^2)$  are the estimated channel errors, which are Gaussian distributed with zero mean and variances  $\sigma_{RSU}^2$  and  $\sigma_{BS}^2$ , respectively. It is supposed that estimated coefficients and errors are uncorrelated.

From Eq. 1, the received SINR of  $\mathcal{V}_{k,i}$  after SIC is as follow.

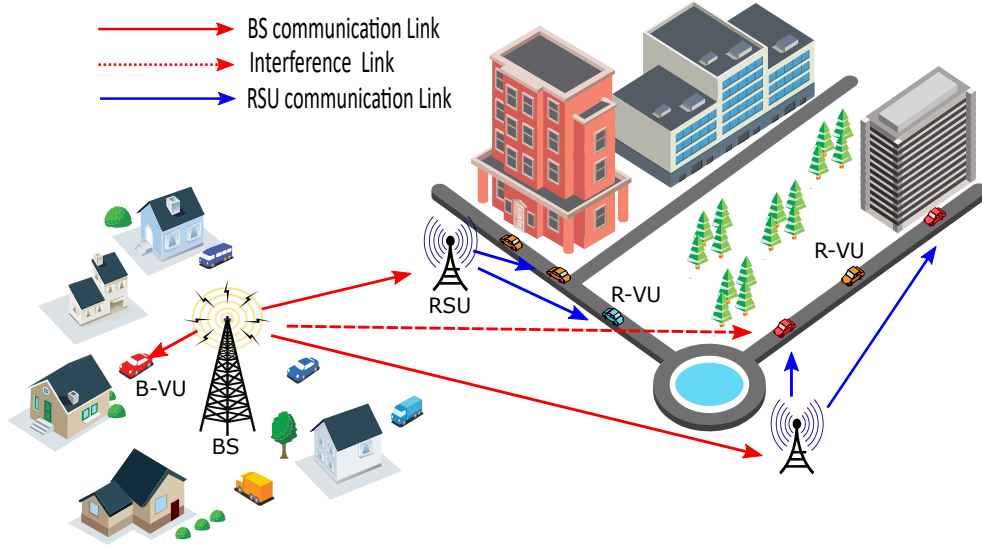


Fig. 1. Illustration of System model

$$\gamma_{k,i} = \frac{P_i \alpha_{k,i} |H_{k,i}|^2}{\underbrace{|H_{k,i}|^2 \sum_{m=k+1}^K P_i \alpha_{m,i}}_{\text{NOMA user interference}} + \underbrace{|G_{k,i}|^2 \sum_{b=1}^B P_b}_{\text{B-VUs Interference}} + \sigma^2}. \quad (7)$$

Under the conditions of perfect CSI, the maximum achievable transmission/data rates of  $\mathcal{V}_{k,i}$  can be written as, respectively.

$$C_{k,i} = BW \log_2(1 + \gamma_{k,i}). \quad (8)$$

Under the conditions of imperfect CSI, the estimated received SINR of  $\mathcal{V}_{k,i}$  is given as

$$\hat{\gamma}_{k,i} = \frac{P_i \alpha_{k,i} |\hat{H}_{k,i}|^2}{\underbrace{|\hat{H}_{k,i}|^2 \sum_{m=k+1}^K P_i \alpha_{m,i}}_{\text{NOMA user interference}} + \underbrace{|\hat{G}_{k,i}|^2 \sum_{b=1}^B P_b}_{\text{B-VUs Interference}} + \sigma^2}. \quad (9)$$

Its corresponding estimated or scheduled data rate can be written as

$$R_{k,i} = BW \log_2(1 + \hat{\gamma}_{k,i}). \quad (10)$$

Under imperfect CSI, the scheduled data transmission rate of vehicles may easily surpass the maximum achievable rate of vehicles, which fails the decoding and successive interference cancellation (SIC) at vehicles. Therefore, outage probability has adopted that measure whether the scheduled rate of vehicles exceeds the maximum achievable rate of vehicles with imperfect CSI. Then, the average outage sum-rate of the  $RSU_i$  can be given as [39]

$$R_i = \sum_{k=1}^K R_{k,i} \cdot Pr[R_{k,i} \leq C_{k,i} | \hat{h}_{k,i}, \hat{g}_{k,i}]. \quad (11)$$

## B. Problem Formulation

Energy-efficient multicasting through multiple RSUs is the primary purpose of the optimization problem. The main objective is to maximize the system sum-rate with the unit power cost. Therefore, the energy efficiency of the system is formulated as the ratio of the sum-rate of the system to the total power consumption of the system. The energy efficiency maximization problem is expressed as

$$\begin{aligned} \max_{P_i, \alpha} \sum_{i=1}^I E_i &= \max_{P_i, \alpha} \sum_{i=1}^I \frac{R_i}{P_i \alpha + P_c}, \\ \text{s.t. } C1 &: Pr[R_{k,i} > C_{k,i} | \hat{h}_{k,i}, \hat{g}_{k,i}] \leq P_{out}, \forall k, i, \\ C2 &: P_i \alpha_{k,i} |\hat{H}_{k,i}|^2 \geq (2^{R_{min}} - 1) \times (|\hat{H}_{k,i}|^2 \\ &\quad \sum_{m=k+1}^K P_i \alpha_{m,i} + |\hat{G}_{k,i}|^2 \sum_{b=1}^B P_b + \sigma^2), \forall k, i, \\ C3 &: P_{low} \leq P_i \leq P_{high}, \forall i, \\ C4 &: \sum_{k=1}^K \alpha_{k,i} \leq 1, \forall k, i, \\ C5 &: \alpha_{k,i} \geq 0, \forall k, i, \end{aligned} \quad (12)$$

where  $E_i$  represents energy efficiency of the  $RSU_i$ .  $\sum_{i=1}^I P_i \alpha$  and  $P_c$  are the transmission power and circuit power consumption, respectively.  $\alpha = \{\alpha_{1,i}, \alpha_{2,i}, \dots, \alpha_{K,i}\}$  is the vector of power allocation factors of vehicles associated with  $RSU_i$ .  $R_i$  is the scheduled sum rate of vehicles associated with  $RSU_i$ .  $C1$  constraint ensure the requirement of channel outage probability ( $P_{out}$ ).  $C2$  guarantees QoS (minimum required rate) provisioning for each vehicle.  $C3$  enforces the transmission power limit of RSUs.  $C4$  constraint describes the condition for power allocation factor of vehicles connected with  $RSU_i$ .  $C5$  ensures that the power assigned to each vehicle is non-negative.

The optimization problem in Eq. (12) can not achieve an optimal global solution under probabilistic constraint  $C1$ ,

which are transformed into a non-probabilistic problem via approximation or relaxation. For instance, The maximum achievable data rate of  $\mathcal{V}_{k,i}$  can be rewritten as

$$C_{k,i} = BW \log_2(1 + \gamma_{k,i}) = BW \log_2\left(1 + \frac{x_{k,i}}{y_{k,i}}\right), \quad (13)$$

where

$$x_{k,i} = P_i \alpha_{k,i} |H_{k,i}|^2, \quad (14)$$

and

$$y_{k,i} = |H_{k,i}|^2 \sum_{m=k+1}^K P_i \alpha_{m,i} + |G_{k,i}|^2 \sum_{b=1}^B P_b + \sigma^2. \quad (15)$$

The scheduled data rate or estimated data rate of  $\mathcal{V}_{k,i}$  can be expressed as

$$R_{k,i} = BW \log_2(1 + \hat{\gamma}_{k,i}) = BW \log_2\left(1 + \frac{\hat{x}_{k,i}}{\hat{y}_{k,i}}\right), \quad (16)$$

where

$$\hat{x}_{k,i} = P_i \alpha_{k,i} |\hat{H}_{k,i}|^2, \quad (17)$$

and

$$\hat{y}_{k,i} = |\hat{H}_{k,i}|^2 \sum_{m=k+1}^K P_i \alpha_{m,i} + |\hat{G}_{k,i}|^2 \sum_{b=1}^B P_b + \sigma^2. \quad (18)$$

According to [39], the outage probability requirements are always satisfied by the strict constraints. The mathematical proof is demonstrated in Appendix A. These strict constraints are presented as follow,

$$Pr[x_{k,i} \leq \hat{x}_{k,i} | \hat{h}_{k,i}, \hat{g}_{k,i}] = \frac{P_{out}}{2}, \quad (19)$$

and

$$Pr[y_{k,i} \geq \hat{y}_{k,i} | \hat{h}_{k,i}, \hat{g}_{k,i}] \leq \frac{P_{out}}{2}. \quad (20)$$

Putting the value of  $x_{k,i}$  from Eq. (14) into the strict constraint described in Eq. (19), we can derive  $\hat{x}_{k,i}$  as follow.

$$\begin{aligned} Pr[P_i \alpha_{k,i} |H_{k,i}|^2 \leq \hat{x}_{k,i} | \hat{h}_{k,i}, \hat{g}_{k,i}] &= \frac{P_{out}}{2} \\ \Rightarrow Pr[P_i \alpha_{k,i} D_{k,i}^2 |h_{k,i}|^2 \leq \hat{x}_{k,i} | \hat{h}_{k,i}, \hat{g}_{k,i}] &= \frac{P_{out}}{2} \\ \Rightarrow Pr[|h_{k,i}|^2 \leq \frac{\hat{x}_{k,i}}{P_i \alpha_{k,i} D_{k,i}^2} | \hat{h}_{k,i}, \hat{g}_{k,i}] &= \frac{P_{out}}{2} \\ \Rightarrow F_{|h_{k,i}|^2}\left(\frac{\hat{x}_{k,i}}{P_i \alpha_{k,i} D_{k,i}^2}\right) &= \frac{P_{out}}{2} \\ \Rightarrow \hat{x}_{k,i} &= F_{|h_{k,i}|^2}^{-1}\left(\frac{P_{out}}{2}\right) P_i \alpha_{k,i} D_{k,i}^2, \end{aligned} \quad (21)$$

where  $|h_{k,i}|^2 \sim CN(\hat{h}_{k,i}, \sigma_{RSU}^2)$  is a random variable with non central chi-squared distribution, which has 2 degrees of freedom.  $F_{|h_{k,i}|^2}$  is its corresponding cumulative distribution function (CDF) while  $F_{|h_{k,i}|^2}^{-1}$  denotes inverse CDF of the non central chi square distribution.

Similarly, we can derive  $\hat{y}_{k,i}$  by substituting the value  $y_{k,i}$  from Eq. (15) into the strict constraint described in Eq. (20) and then applying Markov inequality [43], as follow

$$\begin{aligned} Pr[|H_{k,i}|^2 \sum_{m=k+1}^K P_i \alpha_{m,i} + |G_{k,i}|^2 \sum_{b=1}^B P_b + \sigma^2 \\ \geq \hat{y}_{k,i} | \hat{h}_{k,i}, \hat{g}_{k,i}] &\leq \frac{P_{out}}{2} \\ \Rightarrow Pr[D_{k,i}^2 |h_{k,i}|^2 \sum_{m=k+1}^K P_i \alpha_{m,i} + D_{k,i}^2 |g_{k,i}|^2 \sum_{b=1}^B P_b \\ \geq \hat{y}_{k,i} - \sigma^2 | \hat{h}_{k,i}, \hat{g}_{k,i}] &\leq \frac{P_{out}}{2} \\ E[D_{k,i}^2 |h_{k,i}|^2 \sum_{m=k+1}^K P_i \alpha_{m,i} + D_{k,i}^2 |g_{k,i}|^2 \sum_{b=1}^B P_b] \\ \Rightarrow \frac{E[D_{k,i}^2 |h_{k,i}|^2 \sum_{m=k+1}^K P_i \alpha_{m,i} + D_{k,i}^2 |g_{k,i}|^2 \sum_{b=1}^B P_b]}{\hat{y}_{k,i} - \sigma^2} &= (22) \\ \leq \frac{P_{out}}{2} \\ \Rightarrow \frac{D_{k,i}^2 |h_{k,i}|^2 \sum_{m=k+1}^K P_i \alpha_{m,i} + D_{k,i}^2 |g_{k,i}|^2 \sum_{b=1}^B P_b}{\hat{y}_{k,i} - \sigma^2} \\ = \frac{P_{out}}{2} \\ \Rightarrow \hat{y}_{k,i} &= \frac{2}{P_{out}} \\ (D_{k,i}^2 |g_{k,i}|^2 \sum_{b=1}^B P_b + D_{k,i}^2 |h_{k,i}|^2 \sum_{m=k+1}^K P_i \alpha_{m,i}) + \sigma^2. \end{aligned}$$

Now, the scheduled rate of  $\mathcal{V}_{k,i}$  with the channel outage probability constraint in the form of non-probabilistic form after relaxation or approximation can be written as

$$R_{k,i}^* = BW \log_2(1 + \hat{\gamma}_{k,i}^*), \quad (23)$$

where,  $\hat{\gamma}_{k,i}^*$  is the transformed estimated SINR of the  $\mathcal{V}_{k,i}$ , which can be obtained by inserting the value of  $\hat{x}_{k,i}$  and  $\hat{y}_{k,i}$  from Eq. (21) and Eq. (22) respectively, as follow

$$\begin{aligned} \hat{\gamma}_{k,i}^* &= \frac{\hat{x}_{k,i}}{\hat{y}_{k,i}} \\ &= \frac{F_{|h_{k,i}|^2}^{-1}\left(\frac{P_{out}}{2}\right) P_i \alpha_{k,i} D_{k,i}^2}{\frac{2}{P_{out}} (D_{k,i}^2 |g_{k,i}|^2 \sum_{b=1}^B P_b + D_{k,i}^2 |h_{k,i}|^2 \sum_{m=k+1}^K P_i \alpha_{m,i} + \sigma^2)} \\ &= \frac{P_{out} F_{|h_{k,i}|^2}^{-1}\left(\frac{P_{out}}{2}\right) P_i \alpha_{k,i} D_{k,i}^2}{2(D_{k,i}^2 |h_{k,i}|^2 \sum_{m=k+1}^K P_i \alpha_{m,i} + D_{k,i}^2 |g_{k,i}|^2 \sum_{b=1}^B P_b) + P_{out} \cdot \sigma^2}, \end{aligned} \quad (24)$$

where  $|h_{k,i}|^2 = (|\hat{h}_{k,i}|^2 + \sigma_{RSU}^2)$  and  $|g_{k,i}|^2 = (|\hat{g}_{k,i}|^2 + \sigma_{BS}^2)$ .

The above equation can be rewritten as follow

$$\hat{\gamma}_{k,i}^* = \frac{X_{k,i} P_i \alpha_{k,i}}{Y_{k,i} + Z_{k,i} \sum_{m=k+1}^K P_i \alpha_{m,i}}, \quad (25)$$

where,

$$X_{k,i} = P_{out} F_{|h_{k,i}|^2}^{-1} \left( \frac{P_{out}}{2} \right) D_{k,i}^2, \quad (26)$$

$$Y_{k,i} = 2D_{k,i}^2 (|\hat{g}_{k,i}|^2 + \sigma_{BS}^2) \sum_{b=1}^B P_b + P_{out} \sigma^2, \quad (27)$$

$$Z_{k,i} = 2D_{k,i}^2 (|\hat{h}_{k,i}|^2 + \sigma_{RSU}^2). \quad (28)$$

Following [39], the average sumrate of  $RSU_i$  can be written as

$$R_i^* = (1 - P_{out}) \sum_{k=1}^K R_{k,i}^*. \quad (29)$$

Based on the above approximation, the optimization problem in Eq. (12) can be rewritten as a transformed non-probabilistic optimization problem as follow

$$\begin{aligned} \max_{P_i, \alpha} \sum_{i=1}^I E_i^* &= \max_{P_i, \alpha} \sum_{i=1}^I \frac{R_i^*}{P_i \alpha + P_c}, \\ \text{s.t. } C1: X_{k,i} P_i \alpha_{k,i} &\geq (2^{R_{min}} - 1), \\ &\times (Y_{k,i} + Z_{k,i} \sum_{m=k+1}^K P_i \alpha_{m,i}), \forall k, i, \\ C2: P_{low} &\leq P_i \leq P_{high}, \forall i, \\ C3: \sum_{k=1}^K \alpha_{k,i} &\leq 1, \forall k, i, \\ C4: \alpha_{k,i} &\geq 0, \forall k, i. \end{aligned} \quad (30)$$

The above non-probabilistic optimization problem with respect to  $\alpha_{k,i}$  is still non-convex. Therefore, it is challenging to get a global optimal solution in practice. A low complexity energy-efficient optimal power allocation algorithm is required and essential, which will be designed and addressed in the rest of the paper.

### C. Energy Efficient Multicasting Scheme Design

For the solution of the formulated optimization problem in Eq. (30), firstly, a low complexity GABS algorithm is adopted for the optimal power ( $P_i^*$ ) allocation of the  $RSU_i$ . GABS algorithm is proposed in [40] for link adaptation. Then, the SCA technique is used to transform the non-convex optimization problem of the power allocation factor of vehicles connected with  $RSU_i$  into the CCFP problem. Finally, the CCFP problem is solved through the Dinkelbach method and dual decomposition algorithm.

1) *Power Allocation Scheme for RSUs*: It is evident that maximum energy efficiency for all RSUs can be achieved if each RSU attains its optimal energy efficiency. Therefore, a low complexity GABS algorithm is used, which searches for an optimal  $P^*$  for maximizing  $E(P^*)$ . The global optimality of GABS is ensured by the quasi-concavity of  $E(P^*)$  [44].

The optimization problem for optimal power allocation for

RSUs can be formulated as follow.

$$\begin{aligned} \max_P \sum_{i=1}^I E_i^* &= \max_P \sum_{i=1}^I \frac{(1 - P_{out}) \sum_{k=1}^K R_{k,i}^*}{P_i \alpha + P_c}, \\ \text{s.t. } C1: P_{low} &\leq P_i \leq P_{high}, \forall i. \end{aligned} \quad (31)$$

For simplicity, the objective function in the above optimization problem for the  $RSU_i$  can be rewritten as

$$E_i^* = \frac{(1 - P_{out}) \sum_{k=1}^K R_{k,i}^*}{P_i \alpha + P_c} = \frac{(1 - P_{out}) BW}{P_i \alpha + P_c} \sum_{k=1}^K \left[ \log_2 \left( 1 + \frac{X_{k,i} P_i \alpha_{k,i}}{Y_{k,i} + Z_{k,i} \sum_{m=k+1}^K P_i \alpha_{m,i}} \right) \right]. \quad (32)$$

$E_i^*$  is strictly quasi-concave with respect to  $P_i$ , which proof is presented in Appendix B. The unique optimal  $P_i^*$  obtained through GABS algorithm should result in  $\frac{\partial E_i^*(P_i)}{\partial P_i} |_{P_i = P_i^*} = 0$ . The detailed GABS algorithm for our problem is presented in Algorithm 1.

As  $E_i^*(P_i)$  is strictly quasi-concave, therefore according to GABS, there is unique  $P_i^*$  such that for any

$$\begin{cases} P_i < P_i^*, & \frac{\partial E_i^*(P_i)}{\partial P_i} > 0; \\ P_i > P_i^*, & \frac{\partial E_i^*(P_i)}{\partial P_i} < 0. \end{cases} \quad (33)$$

Hence, we have the following lemma to seek  $P_i^*$  between two points  $P_{low}$  and  $P_{high}$ , such that  $P_{low} \leq P_i^* \leq P_{high}$ .

**Lemma 1:** Initialize,  $P_i^{[a]} > P_{low}$  and set the step size  $c > 1$ , then for any  $a \geq 0$

$$P_i^{[a+1]} = \begin{cases} P_i^{[a]} c, & \frac{\partial E_i^*(P_i^{[a]})}{\partial P_i^{[a]}} > 0; \\ \frac{P_i^{[a]}}{c}, & \frac{\partial E_i^*(P_i^{[a]})}{\partial P_i^{[a]}} < 0. \end{cases} \quad (34)$$

Repeat Eq. (34) until  $P_i^{[A]}$ , such that  $\frac{\partial E_i^*(P_i^{[A]})}{\partial P_i^{[A]}}$  has a dissimilar sign from  $\frac{\partial E_i^*(P_i^{[0]})}{\partial P_i^{[0]}}$ . Then,  $P_i^*$  must be between  $P_i^{[A]}$  and  $P_i^{[A-1]}$  ( $P_i^{[A-1]} \leq P_i^* \leq P_i^{[A]}$ ). To seek  $P_i^*$  between  $P_i^{[A]}$  and  $P_i^{[A-1]}$ , let  $\hat{P} = \frac{P_i^{[A]} + P_i^{[A-1]}}{2}$ . If  $\frac{\partial E_i^*(\hat{P})}{\partial \hat{P}} = 0$ ,  $P_i^*$  is found. If  $\frac{\partial E_i^*(\hat{P})}{\partial \hat{P}} < 0$ , then replace  $P_i^{[A]}$  with  $\hat{P}$  ( $P_i^{[A-1]} \leq P_i^* \leq \hat{P}$ ). Otherwise, replace  $P_i^{[A-1]}$  with  $\hat{P}$  ( $\hat{P} \leq P_i^* \leq P_i^{[A]}$ ) for  $\frac{\partial E_i^*(\hat{P})}{\partial \hat{P}} > 0$ . This leads to maximum  $E_i^*(P_i^*)$ . GABS algorithm is summarized in detail in Algorithm 1.

GABS converges to the global optimal power  $P_i^*$  in at most  $N_{GABS}$  iterations, where  $N_{GABS} \geq \log_2 \left( \frac{(c-1)P_i^*}{\Delta} - 1 \right)$  [40].  $c$  is the step size, and  $\Delta$  is the maximum tolerance used in Algorithm 1.

2) *Power Allocation Scheme for vehicles with QoS provisioning*: Through GABS optimal power for RSU is obtained. Now the optimization problem for allocating powers to vehicles under QoS constraint can be rewritten as,

**Algorithm 1** GABS for optimal power allocation of RSUs

---

1: **Initialization:** RSU allocates transmit power to each vehicle through NOMA principles without QoS constraint and  $P_i = \frac{P_{low} + P_{high}}{2}$ .

2: Compute  $G_1 = \frac{\partial E_i^*(P_i)}{\partial P_i}$  and  $c > 1$  (step size).

3: **if**  $G_1 > 0$  **then**

4:   **while**  $G_1 > 0$  **do**

5:      $P_i^{(1)} = P_i$  and  $P_i = P_i \times c$

6:     Compute  $G = \frac{\partial E_i^*(P_i)}{\partial P_i}$

7:   **end while**

8: **else**

9:    $P_i^{(1)} = \frac{P_i}{c}$  and compute  $G_2 = \frac{\partial E_i^*(P_i^{(1)})}{\partial P_i^{(1)}}$

10:   **while**  $G_2 < 0$  **do**

11:      $P_i = P_i^{(1)}$  and  $P_i^{(1)} = \frac{P_i^{(1)}}{c}$ .

12:     Compute  $G_2 = \frac{\partial E_i^*(P_i^{(1)})}{\partial P_i^{(1)}}$

13:   **end while**

14: **end if**

15: **while**  $|P_i - P_i^{(1)}| > \Delta$  **do**

16:    $P_i^* = \frac{P_i + P_i^{(1)}}{2}$  and  $\hat{G} = \frac{\partial E_i^*(P_i^*)}{\partial P_i^*}$

17:   **if**  $\hat{G} < 0$  **then**

18:      $P_i = P_i^*$

19:   **else**

20:      $P_i^{(1)} = P_i^*$

21:   **end if**

22: **end while**

23: **Output**  $P_i^*$

---

$$\begin{aligned} \max_{\alpha} \sum_{i=1}^I E_i^* &= \max_{\alpha} \sum_{i=1}^I \frac{R_i^*}{P_i \alpha + P_c}, \\ \text{s.t. } C1: X_{k,i} P_i \alpha_{k,i} &\geq (2^{R_{min}} - 1) \\ &\times (Y_{k,i} + Z_{k,i} \sum_{m=k+1}^K P_i \alpha_{m,i}), \forall k, i, \\ C2: \sum_{k=1}^K \alpha_{k,i} &\leq 1, \forall k, i, \\ C3: \alpha_{k,i} &\geq 0, \forall k, i. \end{aligned} \quad (35)$$

The above optimization problem is non-convex respect to  $\alpha_{k,i}$ . Its objective function has a non-linear fractional form, which is very challenging to solve. Successive convex approximation (SCA) is adopted, reducing complexity and transforming the optimization problem into tractable concave-convex fractional programming (CCFP) problem. SCA in each iteration approximate the non-convex objective function by logarithmic approximation [45] as follow

$$\Pi \log_2(SINR) + \Phi \leq \log_2(1 + SINR), \quad (36)$$

where  $\Pi = \frac{SINR_0}{1 + SINR_0}$  and  $\Phi = \log_2(1 + SINR_0) - \frac{SINR_0}{1 + SINR_0} \log_2(SINR_0)$ . When  $SINR = SINR_0$ , the bound becomes tight. By using the lower bound of inequality in Eq. (36), the data rate of vehicle  $k$  associated with  $RSU_i$  can be

given as

$$\bar{R}_{k,i}^* = BW(\Pi_{k,i} \log_2(\hat{\gamma}_{k,i}^*) + \Phi_{k,i}), \quad (37)$$

where

$$\Pi_{k,i} = \frac{\hat{\gamma}_{k,i}^*}{1 + \hat{\gamma}_{k,i}^*}, \quad (38)$$

and

$$\Phi_{k,i} = \log_2(1 + \hat{\gamma}_{k,i}^*) - \frac{\hat{\gamma}_{k,i}^*}{1 + \hat{\gamma}_{k,i}^*} \log_2(\hat{\gamma}_{k,i}^*). \quad (39)$$

Now the average sumrate of  $RSU_i$  can be rewritten as

$$\bar{R}_i^* = (1 - P_{out}) \sum_{k=1}^K \bar{R}_{k,i}^*. \quad (40)$$

Hence the updated optimization problem can be formulated as

$$\begin{aligned} \max_{\alpha} \sum_{i=1}^I \bar{E}_i^* &= \max_{\alpha} \sum_{i=1}^I \frac{\bar{R}_i^*}{P_i \alpha + P_c}, \\ \text{s.t. } C1: X_{k,i} P_i \alpha_{k,i} &\geq (2^{\frac{R_{min} - \Phi_{k,i}}{\Pi_{k,i}}}), \\ &\times (Y_{k,i} + Z_{k,i} \sum_{m=k+1}^K P_i \alpha_{m,i}), \forall k, i \\ C2: \sum_{k=1}^K \alpha_{k,i} &\leq 1, \forall k, i, \\ C3: \alpha_{k,i} &\geq 0, \forall k, i. \end{aligned} \quad (41)$$

The objective function in Eq. (41) is still non-convex and is in the form of CCFP. So solving it directly is challenging. This problem can be solved in an affordable complexity through Dinkelbach's algorithm [46]. Let  $q = \frac{\bar{R}_i^*}{P_i \alpha + P_c}$ , then the fractional objective function in Eq. (41) can be presented in parametric form as  $F(q) = \bar{R}_i^* - q(P_i \alpha + P_c)$ , where  $q$  is a real parameter. Finding the roots of the  $F(q)$  is equivalent to solving the fractional objective function in Eq. (41) [47],[48]. Now the objective function in Eq. (41) can be written as

$$\max_{\alpha} \sum_{i=1}^I \bar{E}_i^* = \max_{\alpha} \sum_{i=1}^I F(q) = \max_{\alpha} \sum_{i=1}^I \bar{R}_i^* - q(P_i \alpha + P_c). \quad (42)$$

Form Eq. (42),  $F(q)$  is negative when  $q$  approaches infinity, while  $F(q)$  is positive when  $q$  approaches minus infinity.  $F(q)$  is convex about  $q$ . The convex problem in Eq. (42) is solved by adopting the Lagrangian dual decomposition method. The Lagrangian function can be written as

$$\begin{aligned} L(\alpha, \mu, \lambda) &= \frac{(1 - P_{out})BW}{P_i + P_c} \\ &\left( \sum_{k=1}^K \Pi_{k,i} \times \log_2 \left( \frac{X_{k,i} P_i \alpha_{k,i}}{Y_{k,i} + Z_{k,i} \sum_{m=k+1}^K P_i \alpha_{m,i}} \right) + \Phi_{k,i} \right) \\ &- q(P_i \alpha + P_c) + \sum_{k=1}^K \mu_k (X_{k,i} P_i \alpha_{k,i} - 2^{\frac{R_{min} - \Phi_{k,i}}{\Pi_{k,i}}}) \\ &\times (Y_{k,i} + Z_{k,i} \sum_{m=k+1}^K P_i \alpha_{m,i}) + \lambda (1 - \sum_{k=1}^K \alpha_{k,i}), \end{aligned} \quad (43)$$

where  $\boldsymbol{\mu} = \{\mu_1, \dots, \mu_K\}$  and  $\lambda$  are the dual variables or Lagrange multipliers.  $\boldsymbol{\mu}$  is related to the constraint C1 while  $\lambda$  is corresponding to the constraint C2 in Eq. (41). For optimizing the power allocation for the vehicles, constraints are the KKT conditions [49]. The Lagrangian dual function is given by

$$g(\boldsymbol{\mu}, \lambda) = \max_{\alpha > 0, \boldsymbol{\mu}, \lambda \geq 0} L(\alpha, \boldsymbol{\mu}, \lambda) \quad (44)$$

Then, the dual Lagrangian problem is formulated by

$$\min_{\boldsymbol{\mu}, \lambda \geq 0} g(\boldsymbol{\mu}, \lambda), \quad (45)$$

For the given energy efficiency  $q$  and fixed Lagrangian multipliers, its standard optimization problem is based on KKT conditions. The closed-form expression of optimal power allocation factor of  $k^{th}$  vehicle associated with  $RSU_i$  can be derived in Appendix C as

$$\alpha_{k,i} = \frac{(1 - P_{out})BWP_{k,i}}{\ln 2(qP_i + \lambda - \mu_{k,i}(X_{k,i}P_i)) + \sum_{l=1}^{k-1} \Theta(\alpha_{l,i})}, \quad (46)$$

where

$$\Theta(\alpha_{l,i}) = (1 - P_{out})BWP_{l,i} \hat{\gamma}_{l,i}^* \times \frac{Z_{l,i}}{X_{l,i} \alpha_{l,i}} + \ln 2 \mu_{l,i} (Z_{l,i} P_i 2^{\frac{R_{min} - \Phi_{l,i}}{B_{l,i}}}). \quad (47)$$

To utilize the all optimal transmit power of RSU ( $P_i^*$ ) among its connected vehicles, the vehicle with lowest SINR can get its power allocation factor by  $\alpha_{1,i} = 1 - \sum_{k=2}^K \alpha_{k,i}$ . Given the optimal power allocation policy in Eq. (46), the primal problem's dual variables can be computed and updated iteratively by the sub-gradient method [50].

$$\lambda(iter + 1) = [\lambda(iter) - \omega_1(iter)(1 - \sum_{k=1}^K \alpha_{k,i})]^+ \quad (48)$$

$$\mu_{k,i}(iter + 1) = [\mu_{k,i}(iter) - \omega_2(iter)(X_{k,i}P_i \alpha_{k,i} - (2^{\frac{R_{min} - \Phi_{k,i}}{B_{k,i}}})) \times (Y_{k,i} + Z_{k,i} \sum_{m=k+1}^K P_i \alpha_{m,i})]^+ \forall k, i \quad (49)$$

where  $iter$  denotes the iteration index.  $\omega_1$  and  $\omega_2$  are positive step sizes. The appropriate step size is necessary for the convergence of the iteration process to an optimal solution. The iterative power allocation algorithm for vehicles based on Dinkelbach's algorithm is presented in Algorithm 2.

### III. SIMULATION RESULTS

Simulation results are demonstrated in this section to evaluate the efficacy of the proposed energy-efficient multicasting scheme for NOMA 5G V2X communications. The global optimal power allocation for multicasting can be acquired through an exhaustive search [28], which is served as a benchmark. The computational complexity of exhaustive search algorithm is exponential because it is determined by the search space of all possible combinations of power allocation factor of users and the complexity at each search [29]. Therefore, it is not practical for a network with a large number of users. Instead, our proposed algorithm (GABS-Dinkelbach) achieves very close EE to exhaustive search with very low computational

**Algorithm 2** Iterative method based on Dinkelbach's algorithm for optimal power allocation to vehicles under QoS provisioning

- 1: **Initialization:** Assign the energy efficiency obtain through GABS(Algorithm 1), maximum iterations  $N_{max}$ , and maximum tolerance  $\delta_{max}$ . Initialize the dual variables( $\boldsymbol{\mu}$  and  $\lambda$ ) and iteration index  $n = 1$ .
- 2: **while**  $n \leq N_{max}$  **or**  $|\bar{R}_i^*(n) - q(n)(P_i \alpha(n) + P_c)| \geq \delta_{max}$  **do**
- 3:   Compute  $\bar{R}_i^*(n)$  by using Eq. (40)
- 4:   Compute  $q(n) = \frac{\bar{R}_i^*(n)}{P_i \alpha(n) + P_c}$
- 5:   Update dual variables  $\lambda(n)$  and  $\boldsymbol{\mu}(n)$  by using Eq. (48) and (49), respectively.
- 6:   Update the power allocation factor vector  $\alpha(n+1)$  of vehicles by using equation (46)
- 7:    $n = n + 1$ .
- 8: **end while**
- 9: **Output:** Optimal  $\alpha^* = \{\alpha_{1,i}^*, \alpha_{2,i}^*, \dots, \alpha_{K,i}^*\}$

TABLE I  
SIMULATION PARAMETERS

Parameter	Value
Bandwidth	10 MHz
BS Radius	500 m
RSU Radius	30 m
Noise power ( $\sigma^2$ )	-114 dBm
Transmit power of BS ( $P_b$ )	40 dBm
Transmit power of RSU ( $P_i$ )	15 dBm - 30 dBm
Circuit power consumption ( $P_c$ )	30 dBm
Vehicles minimum data rate $R_{min}$	1.5 bps/Hz
Vehicle drop model	spatial Poisson process
Vehicle speed (v)	60 km/h
Vehicle density	2.5v, v in m/s
Pathloss model	$128.1 + 37.6 \log_{10}(d)$ d in km
Shadowing distribution	Log-normal
Shadowing standard deviation	8 dB
Fast fading	Rayleigh fading

complexity, which can be observed from its convergence in Fig. 3. For our simulations, vehicles connected with each RSU are generated by a spatial Poisson process, with a density decided by the vehicle speed. In our simulations, each RSU is serving three vehicles through NOMA, which are selected randomly from the generated vehicles. The minimum distance between BS and vehicles associated with RSU is assumed to be 250. The other main simulation parameters are listed in table I.

Fig. 2 presents the EE of RSU versus the transmit power of RSU in dBm, in which  $\sigma_{RSU}^2 = 0.01$ ,  $\sigma_{BS}^2 = 0.1$  and  $P_{out} = 0.05$ . From the figure, it can be observed that EE as a function of  $P_i$  first increases and then decreases and is quasi concave with regards to  $P_i$ . Therefore, optimal  $P_i$  can be obtained through the GABS algorithm, which achieves optimal EE and is presented by the black circle. During the GABS algorithm, the power allocation factor of vehicles connected with RSU is chosen randomly using the NOMA principle without vehicles' QoS constraints. To satisfy the QoS constraints of the vehicle, the RSU with optimal  $P_i^*$  is



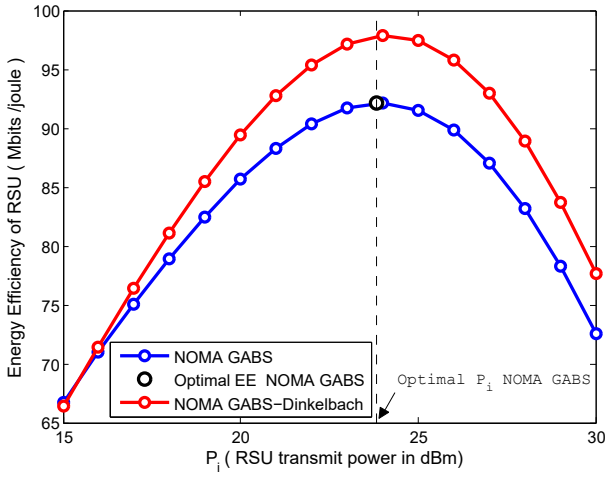


Fig. 2. Energy efficiency of GABS and GABS-Dinkelbach versus RSU transmit powers in dBm

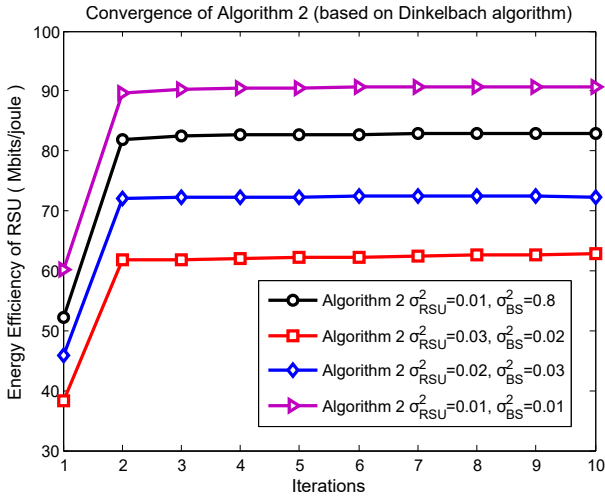


Fig. 3. Energy efficiency Convergence of Algorithm 2 versus number of iterations with different  $\sigma_{RSU}^2$  and  $\sigma_{BS}^2$

used to provide the energy-efficient power allocation factor to vehicles under their QoS constraint through Dinkelbach's algorithm, which is named as GABS-Dinkelbach algorithm. GABS-Dinkelbach has optimal EE under optimal  $P_i^*$ .

In Fig. 3, EE convergence of Algorithm 2 versus iterations is displayed with different  $\sigma_{RSU}^2$  and  $\sigma_{BS}^2$ , where  $P_{out} = 0.05$ . The obtained result shows that Algorithm 2 usually converges in three iterations regardless of channel estimation error variances. It is noted that  $\sigma_{RSU}^2$  and  $\sigma_{BS}^2$  influence EE, but their effect on the convergence of Algorithm 2 is almost negligible.

Fig. 4 compares the EE of the proposed NOMA GABS-Dinkelbach algorithm with optimal GABS-Exhaustive algorithm (high computational complexity) and OFDMA. The comparison is done with different  $\sigma_{RSU}^2$  and  $\sigma_{BS}^2$ , where  $P_{out} = 0.05$ . The proposed algorithm achieves very close EE performance to the optimal NOMA GABS-Exhaustive algorithm with very low computational complexity. Moreover, it can be noticed that higher channel error variances reduce the EE. From the results, it can be analyzed that  $\sigma_{RSU}^2$  has a greater influence on EE as compare to  $\sigma_{BS}^2$ .

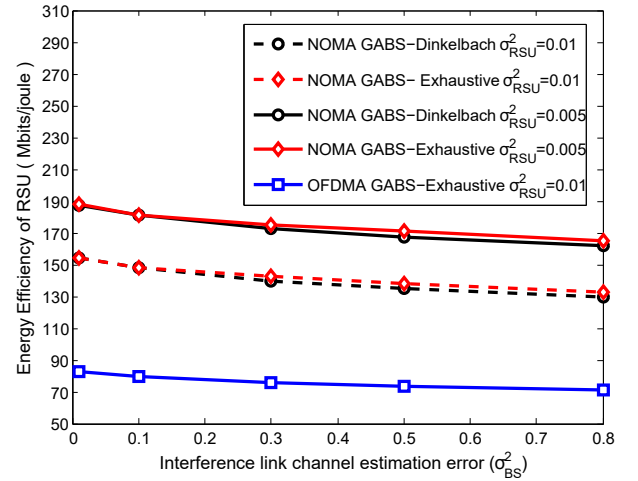


Fig. 4. Energy efficiency of RSU with different transmission link channel error variances ( $\sigma_{RSU}^2$ ) versus interference link channel error variances ( $\sigma_{BS}^2$ )

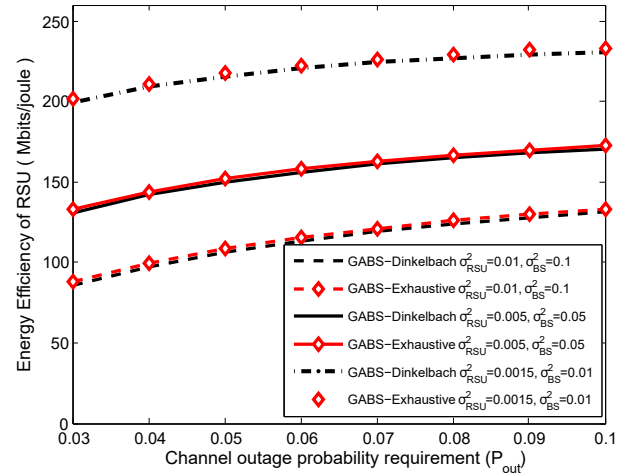


Fig. 5. Energy efficiency of RSU versus  $P_{out}$  with different  $\sigma_{RSU}^2$  and  $\sigma_{BS}^2$

Fig. 5 demonstrates the total EE of the proposed GABS-Dinkelbach algorithm versus channel outage probability requirement with different  $\sigma_{RSU}^2$  and  $\sigma_{BS}^2$ . The proposed method shows very close performance with the optimal GABS-Exhaustive algorithm. Moreover, a higher channel outage probability requirement of the system results in higher EE performance. It can be inspected from the figure that  $\sigma_{RSU}^2$  has a more significant influence on EE compared to  $\sigma_{BS}^2$ .

Fig. 6 depicts EE of proposed algorithm 2 (based on Dinkelbach algorithm) versus the transmit power of RSU in dBm with different  $\sigma_{RSU}^2$  and  $\sigma_{BS}^2$ , where  $P_{out} = 0.05$ . EE first increases and then decreases with increasing  $P_i$ . The reason is that when  $P_i$  is increased beyond the optimal  $P_i^*$ , the RSU sum-rate rises very slowly as compared to the power consumption. It can be examined from the obtained results that proposed GABS-Dinkelbach (Algorithm 1 + Algorithm 2) gets maximum EE (presented by coloured circles) because each RSU transmits with optimal power through algorithm one. Then, algorithm 2 provides the optimal power allocation to

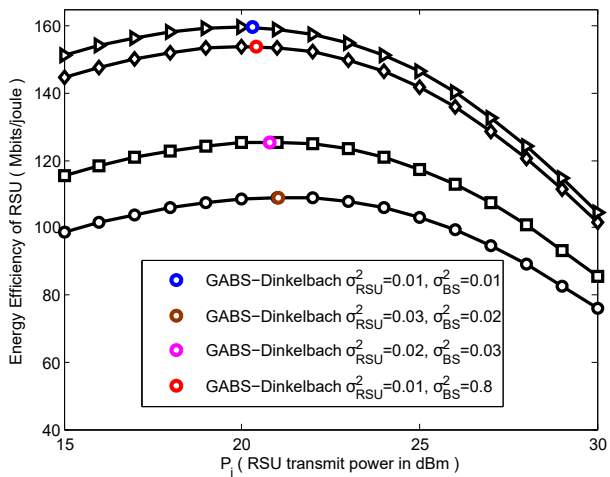


Fig. 6. Energy efficiency of RSU for GABS-Dinkelbach algorithm with different  $(\sigma_{RSU}^2)$  and  $(\sigma_{BS}^2)$  versus  $P_i$  in dBm

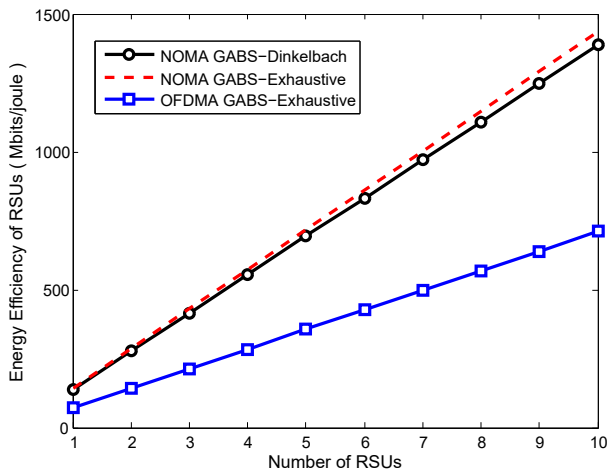


Fig. 7. Energy efficiency of RSUs versus Number of RSUs

the vehicles connected with RSU under their QoS constraints. Furthermore, The EE performance of GABS-Dinkelbach with  $\sigma_{RSU}^2 = 0.02$ ,  $\sigma_{BS}^2 = 0.03$  is higher than its performance with  $\sigma_{RSU}^2 = 0.03$ ,  $\sigma_{BS}^2 = 0.02$ , which indicates that  $\sigma_{RSU}^2$  has a greater influence on the EE of GABS-Dinkelbach algorithm than  $\sigma_{BS}^2$ . Beside it, it can also be seen from the figure that higher channel error variances have higher degradation in the EE of the proposed algorithm.

Fig. 7 shows the energy efficiency of RSUs versus number of RSUs, in which  $\sigma_{RSU}^2 = 0.01$ ,  $\sigma_{BS}^2 = 0.1$  and  $P_{out} = 0.05$ . The number of RSUs increases from 1 to 10. It can be examined that NOMA GABS-Dinkelbach attains very close performance to the optimal NOMA GABS-Exhaustive algorithm. It can also be noticed that EE is increasing monotonously with the increase in the number of RSUs. It is due to the fact that there is no interference among RSUs and higher EE can be obtained with a larger number of RSUs.

Fig. 8 presents the sum rate of RSUs versus number of RSUs, in which  $\sigma_{RSU}^2 = 0.01$ ,  $\sigma_{BS}^2 = 0.1$  and  $P_{out} = 0.05$ . The improvement in the sum-rate of the RSUs through the proposed NOMA GABS-Dinkelbach algorithm is very close

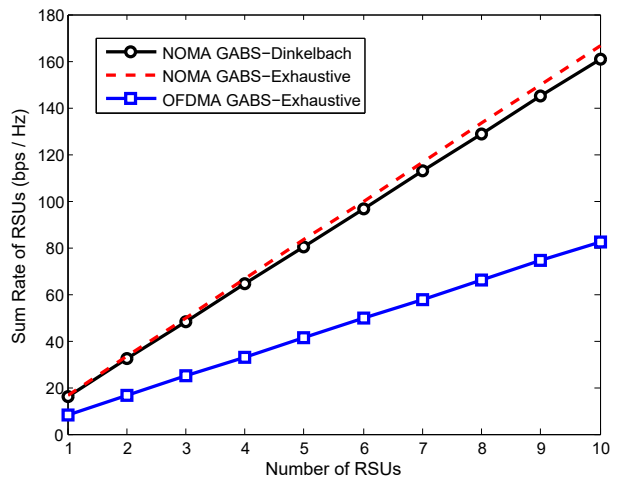


Fig. 8. Sum Rate of RSUs versus Number of RSUs

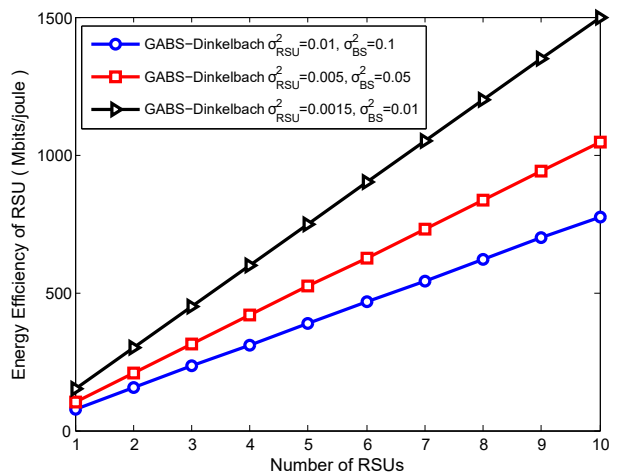


Fig. 9. Energy efficiency of RSUs with different  $(\sigma_{RSU}^2)$  and  $(\sigma_{BS}^2)$  versus Number of RSUs

to the optimal NOMA GABS-Exhaustive algorithm. It can be noticed that the performance gap between the proposed NOMA GABS-Dinkelbach and OFDMA GABS-Exhaustive widens, as the number of RSU grows up.

In Fig. 9, the EE of proposed NOMA GABS-Dinkelbach versus the number of RSUs is presented with different  $\sigma_{RSU}^2$  and  $\sigma_{BS}^2$ , where  $P_{out} = 0.05$ . This figure expresses that the proposed algorithm has higher EE with smaller channel error variances.

#### IV. CONCLUSION

In this paper, a novel low-complexity energy-efficient power allocation algorithm is developed for the 5G V2X system. In which each RSU in the network achieves optimal transmit power through the GABS method under its transmit power limits and channel outage probability requirement of vehicles under imperfect CSI. The probabilistic optimization problem under channel outage probability constraint is converted into a non-probabilistic problem through relaxation. Then, the non-convex power allocation optimization problem of vehicles connected with their corresponding RSU under their QoS

constraint is transformed into a tractable CCFP problem through the SCA technique. The closed-form expressions of power allocation of vehicles are derived where the maximum vehicles can be higher than two on a subchannel. The CCFP problem is solved efficiently through Dinkelbach and the dual decomposition method. The efficacy of the proposed algorithm is verified through simulations, which shows that the proposed algorithm can achieve an optimal solution with very low-complexity as compare to the global optimal exhaustive search algorithm, which obtains optimality with exponential computational complexity. In the future, it would be interesting to expand our work for full-duplex (FD) RSUs, and explore our proposed method as a cooperative NOMA multicasting scheme.

## APPENDIX A

### PROOF OF CHANNEL OUTAGE PROBABILITY REQUIREMENTS IN TERM OF STRICT CONSTRAINTS

Here, we will prove that the channel outage probability constraint C1 in Eq. (12) can be derived from strict constraints described in Eq. (19) and (20).

The constraint C1 for vehicle k from Eq. (12) is given as follow

$$Pr[R_{k,i} > C_{k,i} | \hat{h}_{k,i}, \hat{g}_{k,i}] \leq P_{out},$$

which can be bounded as follow

$$Pr[\hat{y}_{k,i} > \gamma_{k,i} | \hat{h}_{k,i}, \hat{g}_{k,i}] \leq P_{out}. \quad (50)$$

From Eq. (13) and (16), it can be written as

$$Pr\left[\frac{\hat{x}_{k,i}}{\hat{y}_{k,i}} > \frac{x_{k,i}}{y_{k,i}} | \hat{h}_{k,i}, \hat{g}_{k,i}\right] \leq P_{out}. \quad (51)$$

From Eq. (16), it can be derived as

$$\hat{y}_{k,i} = \frac{\hat{x}_{k,i}}{\hat{y}_{k,i}} = 2^{\frac{R_{k,i}}{BW}} - 1. \quad (52)$$

From Eq. (51) and (52),

$$Pr\left[2^{\frac{R_{k,i}}{BW}} - 1 > \frac{x_{k,i}}{y_{k,i}} | \hat{h}_{k,i}, \hat{g}_{k,i}\right] \leq P_{out}. \quad (53)$$

The above outage probability based on total probability theorem can be presented as follow

$$\begin{aligned} & Pr[x_{k,i} \leq \hat{x}_{k,i} | \hat{h}_{k,i}, \hat{g}_{k,i}] \\ & \times Pr\left[2^{\frac{R_{k,i}}{BW}} - 1 > \frac{x_{k,i}}{y_{k,i}} | x_{k,i} \leq \hat{x}_{k,i}, \hat{h}_{k,i}, \hat{g}_{k,i}\right] \\ & + Pr[x_{k,i} > \hat{x}_{k,i} | \hat{h}_{k,i}, \hat{g}_{k,i}] \\ & \times Pr\left[2^{\frac{R_{k,i}}{BW}} - 1 > \frac{x_{k,i}}{y_{k,i}} | x_{k,i} > \hat{x}_{k,i}, \hat{h}_{k,i}, \hat{g}_{k,i}\right] \\ & \leq P_{out} \end{aligned} \quad (54)$$

From Eq. (52),  $\hat{y}_{k,i} = \frac{\hat{x}_{k,i}}{2^{\frac{R_{k,i}}{BW}} - 1}$ . Inserting it into Eq. (20) results in

$$\begin{aligned} & Pr[y_{k,i} \geq \hat{y}_{k,i} | \hat{h}_{k,i}, \hat{g}_{k,i}] \\ & = Pr\left[y_{k,i} \geq \frac{\hat{x}_{k,i}}{2^{\frac{R_{k,i}}{BW}} - 1} | \hat{h}_{k,i}, \hat{g}_{k,i}\right] \\ & = Pr\left[2^{\frac{R_{k,i}}{BW}} - 1 \geq \frac{\hat{x}_{k,i}}{y_{k,i}} | \hat{h}_{k,i}, \hat{g}_{k,i}\right] \leq \frac{P_{out}}{2}. \end{aligned} \quad (55)$$

Based on Eq. (55), when  $x_{k,i} > \hat{x}_{k,i}$ , we can always have

$$\begin{aligned} & Pr\left[2^{\frac{R_{k,i}}{BW}} - 1 > \frac{x_{k,i}}{y_{k,i}} | x_{k,i} > \hat{x}_{k,i}, \hat{h}_{k,i}, \hat{g}_{k,i}\right] \\ & \leq Pr\left[2^{\frac{R_{k,i}}{BW}} - 1 > \frac{\hat{x}_{k,i}}{y_{k,i}} | x_{k,i} > \hat{x}_{k,i}, \hat{h}_{k,i}, \hat{g}_{k,i}\right] \leq \frac{P_{out}}{2}. \end{aligned} \quad (56)$$

From Eq. (19), we can write

$$Pr[x_{k,i} > \hat{x}_{k,i} | \hat{h}_{k,i}, \hat{g}_{k,i}] = 1 - \frac{P_{out}}{2}. \quad (57)$$

Note that

$$Pr\left[2^{\frac{R_{k,i}}{BW}} - 1 > \frac{x_{k,i}}{y_{k,i}} | x_{k,i} \leq \hat{x}_{k,i}, \hat{h}_{k,i}, \hat{g}_{k,i}\right] \leq 1. \quad (58)$$

As Eq. (54) is an equivalent form of constraint C1. Therefore, by putting values from Eq. (19), (58), (57) and (56) in Eq. (54), we have

$$\begin{aligned} \text{The left side of (54)} & \leq 1 \left(\frac{P_{out}}{2}\right) + \left(1 - \frac{P_{out}}{2}\right) \left(\frac{P_{out}}{2}\right) \\ & = -\frac{P_{out}}{4} + P_{out} \approx P_{out}, \end{aligned} \quad (59)$$

for  $P_{out} \ll 1$ .

## APPENDIX B

### PROOF OF $E_i^*$ BEING STRICTLY QUASI-CONCAVE WITH RESPECT TO $P_i$

The objective is to demonstrate that  $E_i^*$  is strictly quasi-concave for  $P_i$ . For strictly quasi concave functions, if the local maximum exists, it is also globally optimal [51]. According to definition, a function is quasi concave if its super level set for any arbitrary real  $\tau$  is strictly convex [52]. For  $E_i^*$ , the super level set is

$$S_\tau = \{P_i \geq 0 | E_i^*(P_i) \geq \tau\}. \quad (60)$$

When  $\tau < 0$ , there is no point that can satisfy  $E_i^*(P_i) = \tau$ . When  $\tau = 0$ , only  $P_i = 0$  can satisfy  $E_i^*(P_i) = \tau$ . It can be seen for  $\tau < 0$ ,  $S_\tau$  is convex because by definition if  $f(x) \leq 0$ , the super level set is convex. For  $\tau > 0$ , the super level set is given as

$$S_\tau = \{P_i \geq 0 | \tau(P_c + P_i) - R_i^* \leq 0\}. \quad (61)$$

Since  $R_i^*$  is strictly concave with respect to  $P_i$  because its second derivative is always negative (the first and second derivative of  $R_i^*$  with respect to  $P_i$  are given in Eq. (62) and (63), respectively). Therefore  $-R_i^*$  is strictly convex in terms of  $P_i$ . Therefore  $S_\tau$  is strictly convex, and  $E_i^*(P_i)$  is strictly quasi concave.

$$\begin{aligned} \frac{\partial R_i^*}{\partial P_i} & = \left( \sum_{k=1}^{K-1} \frac{X_{k,i} \alpha_{k,i} Y_{k,i}}{\ln(2)(Z_{k,i}(\sum_{m=k+1}^K \alpha_{m,i} P_i) + X_{k,i} \alpha_{k,i} P_i + Y_{k,i}))} \right. \\ & \left. \times \frac{1}{(Z_{k,i}(\sum_{m=k+1}^K \alpha_{m,i} P_i) + Y_{k,i}))} \right) + \frac{X_{K,i} \alpha_{K,i}}{\ln(2)(X_{K,i} \alpha_{K,i} P_i + Y_{K,i})}, \end{aligned} \quad (62)$$

and

$$\frac{\partial^2 R_i^*}{\partial^2 P_i} = \sum_{k=1}^{K-1} \Psi_{k,i} + \left( \frac{-(X_{K,i}\alpha_{K,i})^2}{\ln(2)(X_{K,i}\alpha_{K,i}P_i + Y_{K,i})^2} \right), \quad (63)$$

where

$$\begin{aligned} \Psi_{k,i} &= \frac{-A_{k,i}}{B_{k,i}}, \\ A_{k,i} &= X_{k,i}\alpha_{k,i}Y_{k,i} \left( 2(Z_{k,i} \sum_{m=k+1}^K \alpha_{m,i})^2 P_i + 2Z_{k,i} \right. \\ &\quad \left. (\sum_{m=k+1}^K \alpha_{m,i})(X_{k,i}\alpha_{k,i}P_i + Y_{k,i}) + X_{k,i}\alpha_{k,i}Y_{k,i} \right), \\ B_{k,i} &= \ln(2) \left( Z_{k,i} (\sum_{m=k+1}^K \alpha_{m,i}) P_i + Y_{k,i} \right)^2 \left( Z_{k,i} (\sum_{m=k+1}^K \alpha_{m,i}) P_i \right. \\ &\quad \left. + X_{k,i}\alpha_{k,i}P_i + Y_{k,i} \right)^2, \end{aligned} \quad (64)$$

subsequently, The derivative of  $E_i^*$  with regards to  $P_i$  is given as follow

$$\frac{\partial E_i^*}{\partial P_i} = \frac{\frac{\partial R_i^*}{\partial P_i}(P_i + P_c) - R_i^*}{(P_i + P_c)^2}. \quad (65)$$

#### APPENDIX C

##### DERIVATION OF CLOSED-FORM EXPRESSION OF OPTIMAL POWER ALLOCATION FACTOR OF VEHICLES CONNECTED WITH $RSU_i$

For successful SIC process at receivers, the SINR of vehicles associated with the  $RSU_i$  are ordered as shown in Eq. (1).

When  $k = 1$ , The closed-form equation of  $\alpha_{1,i}$  can be computed as

$$\begin{aligned} \frac{\partial L(\alpha, \mu, \lambda)}{\partial \alpha_{1,i}} &= (1 - P_{out})BW\Pi_{1,i} \frac{1}{\ln 2 \times \alpha_{1,i}} \\ &\quad - qP_i + \mu_{1,i}(X_{1,i}P_i) - \lambda, \end{aligned} \quad (66)$$

and

$$\alpha_{1,i} = \frac{(1 - P_{out})BW\Pi_{1,i}}{\ln 2(qP_i + \lambda - \mu_{1,i}(X_{1,i}P_i))}. \quad (67)$$

When  $k = 2$ , the closed-form solution of  $\alpha_{2,i}$  can be calculated as

$$\begin{aligned} \frac{\partial L(\alpha, \mu, \lambda)}{\partial \alpha_{2,i}} &= (1 - P_{out})BW\Pi_{2,i} \frac{1}{\ln 2 \times \alpha_{2,i}} \\ &\quad - \frac{Z_{1,i}P_i}{\ln 2(Y_{1,i} + Z_{1,i}P_i(\alpha_{3,i} + \alpha_{2,i}))} (1 - P_{out})BW\Pi_{1,i} \\ &\quad - qP_i - \mu_{1,i}(Y_{1,i}P_i 2^{\frac{R_{min}-\Phi_{1,i}}{\Pi_{1,i}}}) + \mu_{2,i}(X_{2,i}P_i) - \lambda = 0. \end{aligned} \quad (68)$$

Then we have

$$\alpha_{2,i} = \frac{(1 - P_{out})BW\Pi_{2,i}}{\ln 2(qP_i + \lambda - \mu_{2,i}(X_{2,i}P_i)) + \Theta(\alpha_{1,i})}, \quad (69)$$

where

$$\begin{aligned} \Theta(\alpha_{1,i}) &= (1 - P_{out})BW\Pi_{1,i}\hat{\gamma}_{1,i}^* \times \frac{Z_{1,i}}{X_{1,i}\alpha_{1,i}} \\ &\quad + \ln 2\mu_{1,i}(Z_{1,i}P_i 2^{\frac{R_{min}-\Phi_{1,i}}{\Pi_{1,i}}}). \end{aligned} \quad (70)$$

When  $k = 3$ , the closed-form expression of  $\alpha_{3,i}$  can be evaluated as

$$\begin{aligned} \frac{\partial L(\alpha, \mu, \lambda)}{\partial \alpha_{3,i}} &= (1 - P_{out})BW\Pi_{3,i} \frac{1}{\ln 2 \times \alpha_{3,i}} \\ &\quad - \frac{Z_{1,i}P_i}{\ln 2(Y_{1,i} + Z_{1,i}P_i(\alpha_{3,i} + \alpha_{2,i}))} (1 - P_{out})BW\Pi_{1,i} \\ &\quad - \frac{Z_{2,i}P_i}{\ln 2(Y_{2,i} + Z_{2,i}P_i(\alpha_{3,i}))} (1 - P_{out})BW\Pi_{2,i} \\ &\quad - qP_i - \mu_{1,i}(Y_{1,i}P_i 2^{\frac{R_{min}-\Phi_{1,i}}{\Pi_{1,i}}}) - \mu_{2,i}(Y_{2,i}P_i 2^{\frac{R_{min}-\Phi_{2,i}}{\Pi_{2,i}}}) \\ &\quad + \mu_{3,i}(X_{3,i}P_i) - \lambda = 0. \end{aligned} \quad (71)$$

Then we have

$$\alpha_{3,i} = \frac{(1 - P_{out})BW\Pi_{3,i}}{\ln 2(qP_i + \lambda - \mu_{3,i}(X_{3,i}P_i)) + \Theta(\alpha_{1,i}) + \Theta(\alpha_{2,i})}. \quad (72)$$

Therefore, by deduction, the closed-form expression for the  $k$ -th vehicle on subchannel can be derived as expressed in Eq. (46).

#### ACKNOWLEDGMENT

The authors would like to thank Shanghai Institute of Advanced Communications and Data Sciences.

#### REFERENCES

- [1] A. Alnasser, H. Sun and J. Jiang, "Recommendation-Based Trust Model for Vehicle-to-Everything (V2X)", *IEEE Internet of Things Journal*, vol. 7, no. 1, pp. 440-450, 2020.
- [2] S. Chen, J. Hu, Y. Shi, Y. Peng, J. Fang, R. Zhao, and L. Zhao, "Vehicle-to-everything (V2X) services supported by LTE-based systems and 5G", *IEEE Communications Standards Magazine*, vol 2, no. 1, pp. 70-76, 2017.
- [3] S. Guo and X. Zhou, "Robust Resource Allocation With Imperfect Channel Estimation in NOMA-Based Heterogeneous Vehicular Networks", *IEEE Transactions on Communications*, vol. 67, no. 3, pp. 2321-2332, 2019.
- [4] IEEE Standard for Information technology—Telecommunications and information exchange between systems Local and metropolitan area networks—Specific requirements - Part 11: wireless LAN Medium Access Control (MAC) and Physical Layer (PHY) Specifications, IEEE Std 802.11-2016 (Revision of IEEE Std 802.11-2012), 2016.
- [5] A. Bazzi, B. M. Masini, A. Zanella and I. Thibault, "On the Performance of IEEE 802.11p and LTE-V2V for the Cooperative Awareness of Connected Vehicles", *IEEE Transactions on Vehicular Technology*, vol. 66, no. 11, pp. 10419-10432, 2017.
- [6] S. Chen, J. Hu, Y. Shi and L. Zhao, "LTE-V: A TD-LTE-Based V2X Solution for Future Vehicular Network", *IEEE Internet of Things Journal*, vol. 3, no. 6, pp. 997-1005, 2016.
- [7] L. Liang, G. Y. Li and W. Xu, "Resource Allocation for D2D-Enabled Vehicular Communications", *IEEE Transactions on Communications*, vol. 65, no. 7, pp. 3186-3197, 2017.
- [8] R. Molina-Masegosa and J. Gozalvez, "LTE-V for Sidelink 5G V2X Vehicular Communications: A New 5G Technology for Short-Range Vehicle-to-Everything Communications", *IEEE Vehicular Technology Magazine*, vol. 12, no. 4, pp. 30-39, 2017.
- [9] 3rd Generation Partnership Project; Technical Specification Group Radio Access Network; Study on LTE-based V2X Services, 3GPP TR 36.885 V2.0.0 (Release 14), 2016.
- [10] P. Belanovic, D. Valerio, A. Paier, T. Zemen, F. Ricciato and C. F. Mecklenbrauker, "On Wireless Links for Vehicle-to-Infrastructure Communications", *IEEE Transactions on Vehicular Technology*, vol. 59, no. 1, pp. 269-282, 2010.

- [11] Y. Ni, J. He, L. Cai, J. Pan and Y. Bo, "Joint Roadside Unit Deployment and Service Task Assignment for Internet of Vehicles (IoV)", *IEEE Internet of Things Journal*, vol. 6, no. 2, pp. 3271-3283, 2019.
- [12] S. S. Husain, A. Kunz, A. Prasad, E. Pateromichelakis and K. Samdanis, "Ultra-High Reliable 5G V2X Communications", *IEEE Communications Standards Magazine*, vol. 3, no. 2, pp. 46-52, 2019.
- [13] Q Wu, GY Li, W Chen, DWK Ng, R Schober, "An overview of sustainable green 5G networks," *IEEE Wireless Communications* vol.24, no. 4, pp.72-80, 2017.
- [14] Q Wu, W Chen, DWK Ng, R Schober, "Spectral and energy-efficient wireless powered IoT networks: NOMA or TDMA?" *IEEE Transactions on Vehicular Technology*, vol. 67, no. 7, pp. 6663-6667, 2018.
- [15] F Wei, W Chen, "Low complexity iterative receiver design for sparse code multiple access," *IEEE Transactions on Communications*, vol. 65, no. 2, pp. 621-634, 2016.
- [16] B. Di, L. Song, Y. Li and Z. Han, "V2X Meets NOMA: Non-Orthogonal Multiple Access for 5G-Enabled Vehicular Networks", *IEEE Wireless Communications*, vol. 24, no. 6, pp. 14-21, 2017.
- [17] Y Wang, W Chen, C Tellambura, "A PAPR reduction method based on artificial bee colony algorithm for OFDM signals," *IEEE transactions on wireless communications*, vol. 9, no. 10, pp. 2994-2999, 2010.
- [18] Y Wang, W Chen, C Tellambura, "Genetic algorithm based nearly optimal peak reduction tone set selection for adaptive amplitude clipping PAPR reduction," *IEEE transactions on broadcasting*, vol. 58, no. 3, pp. 462-471, 2012.
- [19] L Wei, W Chen, "Compute-and-forward network coding design over multi-source multi-relay channels," *IEEE Transactions on Wireless Communications*, vol. 11, no. 9, pp. 3348-3357, 2012.
- [20] G Wang, F Gao, W Chen, C Tellambura, "Channel estimation and training design for two-way relay networks in time-selective fading environments," *IEEE Transactions on Wireless Communications*, vol. 10, no. 8, pp. 2681-2691, 2011.
- [21] J Li, Y Chen, Z Lin, W Chen, B Vucetic, L Hanzo, "Distributed caching for data dissemination in the downlink of heterogeneous networks," *IEEE Transactions on Communications*, vol. 63, no. 10, pp. 3553-3568, 2015.
- [22] B. Di, L. Song, Y. Li and G. Y. Li, "Non-Orthogonal Multiple Access for High-Reliable and Low-Latency V2X Communications in 5G Systems", *IEEE Journal on Selected Areas in Communications*, vol. 35, no. 10, pp. 2383-2397, 2017.
- [23] B. Di, L. Song, Y. Li and G. Y. Li, "NOMA-Based Low-Latency and High-Reliable Broadcast Communications for 5G V2X Services", *GLOBECOM 2017 - 2017 IEEE Global Communications Conference*, Singapore, pp. 1-6, 2017.
- [24] Y. Chen, L. Wang, Y. Ai, B. Jiao and L. Hanzo, "Performance Analysis of NOMA-SM in Vehicle-to-Vehicle Massive MIMO Channels", *IEEE Journal on Selected Areas in Communications*, vol. 35, no. 12, pp. 2653-2666, 2017.
- [25] D. Zhang, Y. Liu, L. Dai, A. K. Bashir, A. Nallanathan and B. Shim, "Performance Analysis of FD-NOMA-Based Decentralized V2X Systems", *IEEE Transactions on Communications*, vol. 67, no. 7, pp. 5024-5036, 2019.
- [26] G. Liu, Z. Wang, J. Hu, Z. Ding and P. Fan, "Cooperative NOMA Broadcasting/Multicasting for Low-Latency and High-Reliability 5G Cellular V2X Communications", *IEEE Internet of Things Journal*, vol. 6, no. 5, pp. 7828-7838, 2019.
- [27] Z. Ding, Z. Yang, P. Fan and H. V. Poor, "On the Performance of Non-Orthogonal Multiple Access in 5G Systems with Randomly Deployed Users", *IEEE Signal Processing Letters*, vol. 21, no. 12, pp. 1501-1505, 2014.
- [28] X. Yu, F. Xu, K. Yu and X. Dang, "Power Allocation for Energy Efficiency Optimization in Multi-User mmWave-NOMA System With Hybrid Precoding", *IEEE Access*, vol. 7, pp. 109083-109093, 2019.
- [29] J. Cui, Y. Liu, Z. Ding, P. Fan and A. Nallanathan, "Optimal User Scheduling and Power Allocation for Millimeter Wave NOMA Systems", *IEEE Transactions on Wireless Communications*, vol. 17, no. 3, pp. 1502-1517, 2018.
- [30] H. Xiao, D. Zhu and A. T. Chronopoulos, "Power Allocation With Energy Efficiency Optimization in Cellular D2D-Based V2X Communication Network", *IEEE Transactions on Intelligent Transportation Systems*, 2019.
- [31] C. Zheng, D. Feng, S. Zhang, X. Xia, G. Qian and G. Y. Li, "Energy Efficient V2X-Enabled Communications in Cellular Networks", *IEEE Transactions on Vehicular Technology*, vol. 68, no. 1, pp. 554-564, 2019.
- [32] Q Wu, M Tao, DWK Ng, W Chen, R Schober, "Energy-efficient resource allocation for wireless powered communication networks," *IEEE Transactions on Wireless Communications* vol. 15, no. 3, pp. 2312-2327, 2015.
- [33] Q Wu, W Chen, M Tao, J Li, H Tang, J Wu, "Resource allocation for joint transmitter and receiver energy efficiency maximization in downlink OFDMA systems," *IEEE Transactions on Communications* vol. 63, no. 2, pp. 416-430, 2014.
- [34] Q Wu, W Chen, DWK Ng, J Li, R Schober, "User-centric energy efficiency maximization for wireless powered communications," *IEEE Transactions on Wireless Communications*, vol. 15, no. 10, pp. 6898-6912, 2016.
- [35] Z. Wang, J. Hu, G. Liu and Z. Ma, "Optimal Power Allocations for Relay-assisted NOMA-based 5G V2X Broadcast/Multicast Communications", *2018 IEEE/CIC International Conference on Communications in China (ICCC)*, Beijing, China, pp. 688-693, 2018.
- [36] X. Ren, Wen Chen, B. Gong, Q. Qin, and L. Gui, "Position-Based Interference Elimination for High Mobility OFDM Channel Estimation in Multi-cell Systems," *IEEE Transactions on Vehicular Technology*, vol. 66, no. 9, pp. 7986-8000, 2017.
- [37] X. Ren, M. Tao, and Wen Chen, "Position-Based ICI Elimination for High-Mobility SIMO OFDM Systems," *IEEE Transactions on Vehicular Technology*, vol. 65, no. 8, pp. 6204-6216, 2016.
- [38] X. Ren, Wen Chen, and M. Tao, "Position-Based Compressed Channel Estimation and Pilot Design for High-Mobility OFDM Systems," *IEEE Transactions on Vehicular Technology*, vol. 64, no. 5, pp. 1918-1929, 2015.
- [39] F. Fang, H. Zhang, J. Cheng, S. Roy and V. C. M. Leung, "Joint User Scheduling and Power Allocation Optimization for Energy-Efficient NOMA Systems With Imperfect CSI", *IEEE Journal on Selected Areas in Communications*, vol. 35, no. 12, pp. 2874-2885, 2017.
- [40] G. Miao, N. Himayat and G. Y. Li, "Energy-efficient link adaptation in frequency-selective channels", *IEEE Transactions on Communications*, vol. 58, no. 2, pp. 545-554, 2010.
- [41] W. Dinkelbach, "On Nonlinear Fractional Programming", *Management Science*, vol. 13, no. 7, pp. 492-498, 1967.
- [42] Y. Sun, D. W. K. Ng, Z. Ding and R. Schober, "Optimal Joint Power and Subcarrier Allocation for Full-Duplex Multicarrier Non-Orthogonal Multiple Access Systems", *IEEE Transactions on Communications*, vol. 65, no. 3, pp. 1077-1091, 2017.
- [43] X. Wang, F. Zheng, P. Zhu and X. You, "Energy-Efficient Resource Allocation in Coordinated Downlink Multicell OFDMA Systems", *IEEE Transactions on Vehicular Technology*, vol. 65, no. 3, pp. 1395-1408, 2016.
- [44] G. Miao and G. Song, "Energy and spectrum efficient wireless network design", Cambridge: Cambridge University Press, 2014.
- [45] J. Papandriopoulos and J. S. Evans, "SCALE: A Low-Complexity Distributed Protocol for Spectrum Balancing in Multiuser DSL Networks", *IEEE Transactions on Information Theory*, vol. 55, no. 8, pp. 3711-3724, 2009.
- [46] K. Shen and W. Yu, "Fractional Programming for Communication Systems—Part I: Power Control and Beamforming", *IEEE Transactions on Signal Processing*, vol. 66, no. 10, pp. 2616-2630, 2018.
- [47] M. R. Zamani, M. Eslami, M. Khorramizadeh and Z. Ding, "Energy-Efficient Power Allocation for NOMA With Imperfect CSI", *IEEE Transactions on Vehicular Technology*, vol. 68, no. 1, pp. 1009-1013, 2019.
- [48] A. Zappone and E. Jorswieck, "Energy efficiency in wireless networks via fractional programming theory", *Foundations and Trends in Communications and Information Theory*, vol. 11, no. 3, pp. 185-396, 2015.
- [49] S. Boyd and L. Vandenberghe, "Convex Optimization", Cambridge University Press, 2004.
- [50] W. U. Khan, F. Jameel, T. Ristaniemi, S. Khan, G. A. S. Sidhu and J. Liu, "Joint Spectral and Energy Efficiency Optimization for Downlink NOMA Networks", *IEEE Transactions on Cognitive Communications and Networking*, vol. 6, no. 2, pp. 645-656, 2020.
- [51] H. Zhang, H. Liu, J. Cheng and V. C. M. Leung, "Downlink Energy Efficiency of Power Allocation and Wireless Backhaul Bandwidth Allocation in Heterogeneous Small Cell Networks," *IEEE Transactions on Communications*, vol. 66, no. 4, pp. 1705-1716, 2018.
- [52] F. Alavi, K. Cumanan, Z. Ding and A. G. Burr, "Beamforming Techniques for Nonorthogonal Multiple Access in 5G Cellular Networks," *IEEE Transactions on Vehicular Technology*, vol. 67, no. 10, pp. 9474-9487, 2018.